

# A unified algorithm framework for quality control of sensor data for behavioural clinimetric testing

Reham Badawy<sup>1\*</sup>, Yordan Raykov<sup>1\*</sup>, Max A. Little<sup>1,2</sup>

**Abstract**—The use of smartphone and wearable sensing technology for objective, non-invasive and remote clinimetric testing of symptoms has considerable potential. However, the clinimetric accuracy achievable with such technology is highly reliant on separating the useful from irrelevant or confounded sensor data. Monitoring patient symptoms using digital sensors outside of controlled, clinical lab settings creates a variety of practical challenges, such as unavoidable and unexpected user behaviours. These behaviours often violate the assumptions of clinimetric testing protocols, where these protocols are designed to probe for specific symptoms. Such violations are frequent outside the lab, and can affect the accuracy of the subsequent data analysis and scientific conclusions. At the same time, curating sensor data by hand after the collection process is inherently subjective, laborious and error-prone. To address these problems, we report on a unified algorithmic framework for automated sensor data quality control, which can identify those parts of the sensor data which are sufficiently reliable for further analysis. Algorithms which are special cases of this framework for different sensor data types (e.g. accelerometer, digital audio) detect the extent to which the sensor data adheres to the assumptions of the test protocol for a variety of clinimetric tests. The approach is general enough to be applied to a large set of clinimetric tests and we demonstrate its performance on walking, balance and voice smartphone-based tests, designed to monitor the symptoms of Parkinson’s disease.

## I. INTRODUCTION

**I**N recent years sensors embedded in smartphones and wearable devices have become ubiquitous, and have evolved to the point where they can be used in areas such as healthcare [1, 2, 3], environmental monitoring [4, 5] and transport [6]. In healthcare, for example, smartphone sensors have been successful at detecting the symptoms of neurological disorders such as Parkinson’s disease (PD). PD is a brain disease that significantly affects voluntary movement. Symptoms of PD include slowness of movement (bradykinesia), trembling of the hands and legs (tremor), absence of movement and loss of balance (postural instability). Through a smartphone application, on-board sensors in the smartphone capture the behaviour of the user while they carry out a simple clinimetric test protocol, such as walking in a straight line with the smartphone in their pocket [7], to detect the key symptoms of the disease. Collecting objective symptom measurements with clinimetric testing performed on technologies such as smartphones [8, 9], or portable and wearable sensors [10, 11, 12], eliminates much of the subjective bias of clinical expert symptom measurement, while also allowing for remote, long-term monitoring of

patient health [13]; in contrast to the current “snapshot” in time obtained during a clinical visit. Thus, remote, long-term monitoring allows for improved analysis of a patient’s health and outcomes. Usually, data from such sensors is collected and analysed under a set of clinimetric test protocol assumptions, such as the type of behaviour to be carried out to probe for specific symptoms. Getting the assumptions of a test protocol to hold outside controlled lab settings is a universal problem, since uncontrollable confounding factors in the environment, such as unavoidable and unexpected behaviours, can have an adverse impact on the measurement process.

When the test protocol assumptions do not hold for the sensor data, the interpretation of the analysis results becomes dubious – we are unlikely to be analysing the behaviour we believe we have captured for subsequent symptom measurement. Moreover, analysing confounded or contaminated data produces misleading, biased results which are inherently non-reproducible and non-replicable [14]. In many consumer applications which use sensor technologies, such data collection quality issues may not be that important, but they are of critical importance in the medical sciences. Non-reproducible results in clinimetric studies could have significant implications for an individual’s health.

In clinimetric testing, test protocols are comprised of specific activities (behaviours) that a user is required to perform. This means that the quality control process can be viewed as the problem of locating different user behaviours and assessing if those behaviours are in adherence with the protocol assumptions. Yet it is not feasible to approach this problem using methods used for “activity recognition”, for the following reasons: typically, in activity recognition in “ubiquitous computing” applications, the sensor data is segmented into windows of fixed alignment and equal duration and then a hand-crafted set of features is extracted from each window [15]. Subsequently, these features are used to train a classification algorithm that predicts the activity in each window. One of the problems is that both the hand-engineering of features and the training of the classifier in such systems depends heavily on having detailed, labeled information about which activities actually occurred. However, outside the lab such information is rarely available. The second problem with current approaches to activity recognition, is that usually they rely on modeling the feature space instead of the raw data [16]. This means that often they do not take into account the temporal dependence of the sensor data between windows. These limitations are not reflected in the reported accuracies of these system since they are trained and tested only under controlled lab environments [17, 18, 19, 12].

\*These authors contributed equally to this work.

1. Aston University, UK; 2. Media Lab, Massachusetts Institute of Technology, US

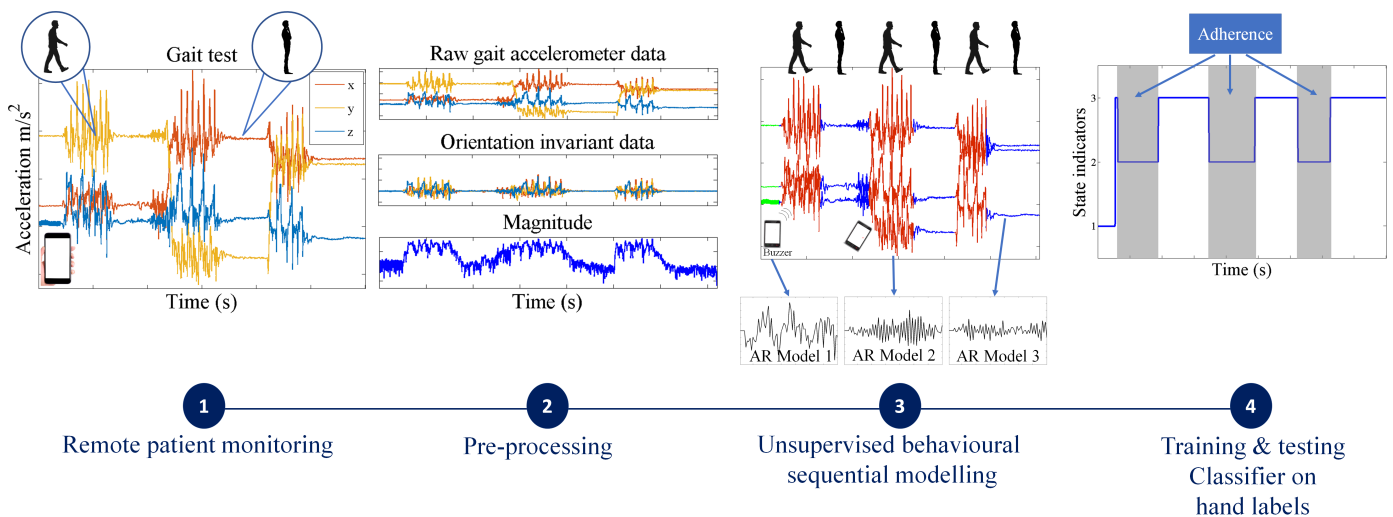


Fig. 1. Overview of the proposed algorithmic framework for data quality control of sensor data for behavioural clinimetric testing. The first stage (starting from the left) involves collecting sensor data outside the lab. The second pre-processing stage consists of removing confounding factors from the data such as the effect of orientation of the device. The third stage involves unsupervised behavioural segmentation of the data into intervals in which the user performs similar activities. In the final stage, a simple, interpretable classifier is trained to predict which behavioural intervals are associated with adherence to, and which with violations of, the test protocols.

Performance of heavily “fine-tuned” machine learning systems for activity recognition are misleading if the sensor data collected outside the lab is drawn from a different distribution to that collected in the lab and used for training the system [20]. This problem is compounded when using high performance nonlinear classification algorithms (such as *convolutional neural networks*, *random forest classifiers* or *support vector machines*) on a large number of features all estimated from a training distribution of questionable relevance in practice.

To address these issues, in this study we propose a unified algorithm framework for automated assessment of clinimetric sensor data quality, i.e. the extent to which the data adheres to the assumptions of the clinimetric test protocols. Combining both parametric and nonparametric signal processing and machine learning techniques we demonstrate the scope, effectiveness and interpretability of this framework by applying it to multiple sensor types and clinimetric tests for assessment of PD. Across 100 participants and 300 clinimetric tests from 3 different types of behavioural clinimetric protocols, the system shows average segmentation accuracy of around 90% when compared to a human expert performing the same quality control task manually. We focus on data collected from smartphone sensors deployed outside the lab, as these are the most ubiquitous devices available for objective symptom measurement in practice.

## II. RELATED WORK

Smartphones and wearables are increasingly recognized as potential tools for remote monitoring, diagnosis and symptom assessment of patients with various conditions: wearable wrist bands have been increasingly used to predict epileptic seizures [21]; smartphones have proven accurate for monitoring of PD symptoms in clinical trials [22]; shoe-based devices have been

developed to support rehabilitation of patients who have suffered through a stroke [23]; and apps have been developed that provide insulin dosage recommendations for type 1 diabetes patients [24]. Many other recent healthcare applications of consumer electronic devices can be found in wider reviews such as Ozdalga et al. [25], Mosa et al. [26] and Kubota et al. [27]. For such devices to become useful clinical tools they have to be deployed in realistic natural environments such as the private home or the office. However, it is difficult to ensure that the same machine learning systems that have been developed in a controlled lab setting can perform well in unknown environmental settings. Training and testing systems on data collected outside of the lab is not really feasible since we have very little labeled information about detailed user behaviours in this situation. Such labels are commonly generated by manual hand labeling by a trained expert, video monitoring of users and user self-assessment. Video recordings are subsequently manually annotated and common in continuous monitoring systems, for example tremor detection [28] or PD disease state assessment [29]. Using video annotations significantly complicates the experimental setup, makes clinimetric studies a lot more expensive and is still quite difficult to analyze. This is why often only certain parts of the video recording are used to obtain labels for parts of the collected data. Alternatively, self-assessment and self-report diaries usually deviate significantly from expert assessment, at least for neurological disorders such as PD [30]. Manual expert annotation of sensor data is also not always objective and typically can provide only broad indications of user behaviour or health status. Unfortunately, these issues are often overlooked, in particular when it comes to the evaluation of clinimetric testing tools and studies often rely only on data captured in the lab [31, 32, 33].

Assuming only some limited amount of labeling is available, in this paper we propose an automated system which aims to recognize deviation between the instructions of the clinimetric

test protocol and the user behaviour, in realistic settings outside the lab environment. Since clinimetric test protocols are expressed in terms of assumptions about the user's behaviour, the quality control algorithms we develop here are related to, but quite different from, existing activity recognition systems. Activity classification frameworks have been used in PD symptom assessment systems [34, 35, 36]. For example, Zwartjes et al. [34] and Salarian et al. [35] developed an in-home monitoring system that detects specific behaviours, and subsequently predicts the movement impairment severity of these activities in terms of common PD symptoms. Both studies use existing activity classification methods which rely upon training on a predefined, specific set of motion-related features which can be used to distinguish between a selected, fixed set of activities. However, it is not feasible in practice to anticipate the entire behavioural repertoire of a participant during any clinimetric test conducted outside the lab. Existing activity recognition systems require a rich set of features to be extracted from the input data and the choice of features depends on the activities we wish to discriminate between [15]. For these reasons most traditional supervised activity recognition systems are not feasible for quality control in the context discussed in this paper, where any set of a potentially infinite range of behaviours could be encountered. A solution to tackling the wide range of possible behaviours in practice is to cluster the data into variable size windows using segmentation, where the specific activity in each segment is not specified. Guo et al. [37] proposed a somewhat more adaptive segmentation approach which does not rely on an a-priori fixed set of features, but uses principal component analysis to select the most appropriate features for the different segmentation tasks. The segmentation of activities is then mostly performed using bottom-up hierarchical clustering on windows of 5 to 10 seconds duration. Hammerla et al. [29] also proposed an approach less reliant on activity-specific features which utilizes a deep belief network with two-layer restricted Boltzmann machines. However, the deep network itself is trained on generic features extracted from 1 minute windows of sensor data, therefore it cannot be used to capture short-term deviations from test protocols.

To design a robust system which can detect short-term deviations from test protocols without relying on hard-to-obtain, detailed labels about the user behaviour during multiple tests, we turn to an unsupervised segmentation approach. Unsupervised time series segmentation methods have been widely studied across many disciplines including: computer vision and graphics [16, 38, 39, 40]; data mining [41]; speech recognition [42, 43] and signal processing [44, 45]. However, most of those techniques cannot be readily applied to low-dimensional sensor data since their usefulness relies on a significant number of domain-specific features.

### III. OVERVIEW

In this section we describe the stages in our proposed unified framework for quality control of clinimetric test sensor data (Figure 1). As an example application we apply the system to multiple clinimetric tests for PD symptom monitoring. We

describe the test protocols for these clinimetric tests in Section IV.

In the first stage, we apply practical preprocessing steps which, depending on the type of sensor produce a more compact representation of the data without discarding any essential structure. For example, in the case of accelerometer data from sensors embedded in smartphones, we can remove the effect of orientation changes of the smartphone. This is because device orientation is usually a confounding factor in clinimetric testing. For high sample-rate voice data we segment the original signal into short duration, 10ms windows and extract features such as the energy or spectral power in each window, instead of modeling the raw data directly. Unlike most of the existing machine learning strategies for processing sensor data we do not rely on a large number of features extracted from each sensor type; we apply minimal transformations to the raw data keeping it at relatively high sampling frequency, and directly fit a flexible probabilistic model aiming to capture the structure of importance to the problem of quality control.

Once the sensor data has been preprocessed accordingly, we fit in an unsupervised manner a discrete latent variable model to each of the sensor signals and use it to split the data into segments of varying duration. Depending on the complexity of the data produced by different clinimetric tests, we propose two different segmentation models which vary in terms of flexibility and computational simplicity:

- 1) For simpler quality control problems, we develop a Gaussian mixture model (GMM) based approach which attempts to cluster the raw signal into two classes: data adhering or not adhering to the test protocols. Since GMMs ignore the sequential nature of the sensor data, we pass the estimated class indicators through a running median filter to smooth out unrealistically frequent switching between the two classes.
- 2) We also propose a more general solution which involves fitting flexible nonparametric switching autoregressive (AR) models to each of these preprocessed sensor signals. The switching AR model segments the data in an unsupervised way into a random (unknown) number of behavioural patterns that are frequently encountered in the data. An additional classifier is then trained to discriminate which of the resulting variable-length segments represent adherence or violation of the test protocol. We demonstrate that a simple multinomial naive Bayes classifier can be trained using a strictly limited amount of labeled data annotated by a human expert. Since the instructions in any clinimetric test protocol are limited, whereas the number of potential behavioural violations of the protocol are not, we assume that any previously unseen segments that we detect have to be a new type of violation to the specified instructions of the protocol. We have detailed the segmentation and classification process in Section VI.

## IV. EXPERIMENTAL SETUP

### A. Data collection

To illustrate our novel framework in practice, we use data from the Smartphone-PD study [46], which utilizes an Android OS smartphone application to capture raw sensor data from the digital sensors embedded in the device. The application prompts the user to undertake short (less than 30 seconds) self-administrated clinimetric tests designed to elicit the symptoms of PD. These tests are: (1) voice test (microphone) which measures impairment in the production of vocal sounds; (2) balance test (accelerometer) which measures balance impairment (postural instability); and (3) walk test (accelerometer) which measures impairment in a user’s walking pattern (Table I).

### B. Hand-labelling for algorithm evaluation

In order to evaluate the performance of the automated quality control algorithms developed here, some reference data is needed. To this end, the data from some of the selected Smartphone tests were hand-labeled according to whether it represents behaviour that adheres to the test protocol or violates it (those labels will later appear as  $u_1, \dots, u_T$  which take value 1 for adherence and value 2 for violation). Note that this is an inherently subjective process and we cannot be sure of the exact activity occurring during any period of time. However, the hand-labelling at least provides an example of how a human expert would classify the collected data. Thus, our aim is not to create an algorithm which blindly reproduces the hand labels as they are imperfect. Instead, we aim to develop an approach that learns the major structural differences between data violating, and data adhering to, test protocols.

We labelled data from 100 subjects (voice, balance and walking tests) from the Smartphone-PD data, randomly selecting 50 PD patients (25 males and 25 females) and 50 healthy controls (25 males and 25 females). Subjects are age and gender-matched (two-sample Kolmogorov-Smirnov test) to rule out potential age or gender confounds (Table I).

We present some illustrative examples of applying our hand-labelling protocol to walking clinimetric test sensor data collected from individuals with PD and healthy individuals. Figure 2(a-b) shows examples in which the user is adhering to the test protocol, i.e. the user is apparently walking throughout the entire duration of the test as instructed. By contrast, in Figure 2(c-d) the user is also walking, however, the smartphone buzzer, which is active for a duration of approximately 2 seconds at the start of the test, is included in the recording.

Figure 2(e-f) shows examples in which the user deviates from the test protocol near the end of the test (e), and midway through the test (f). The noticeable gap in walking for the PD patient in test (e) may be due to “freezing of gait” (an absence of movement despite the intention to walk), an important PD symptom. Nonetheless, we favour removing such instances from the data as without additional information we cannot be sure of this identification.

Figure 2(g-h) shows examples in which the user is not adhering to the test protocol throughout the duration of the

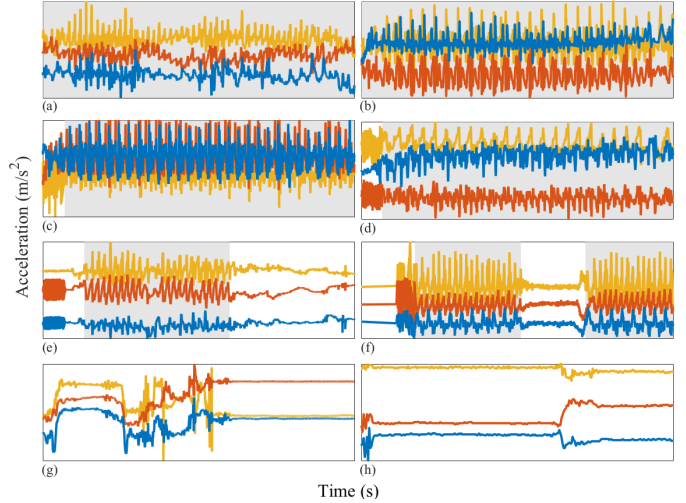


Fig. 2. Illustrative examples of walking clinimetric test sensor data recorded using a smartphone accelerometer from healthy individuals and those with Parkinson’s disease. Left column: walking tests from PD patients, right column: healthy individuals. Horizontal axis: time in seconds (approximately 30s), vertical axis (orange, red and blue) represents acceleration (m/s). Grey shaded areas: data segments in which the user is hand-labelled as adhering to the test protocol. (a) PD patient walking throughout test, (b) healthy individual walking throughout test, (c) smartphone buzzer in first few seconds of test, PD patient walking throughout test, (d) buzzer recorded in first few seconds of test, healthy individual walking throughout test, (e) buzzer recorded in the first few seconds of test, PD patient deviates from test protocol before adhering to test instructions by starting to walk, near the end of the test, PD patient deviates from test protocol, (f) buzzer captured in the first few seconds of test, healthy individual then begins walking, after which individual deviates from test protocol and resumes walking near end of test, (g-h) PD patient and healthy individual both deviate from test instructions throughout the test.

test. Such instances can occur, for example, when the user is attempting the test for the first time, or when the user is interrupted at the start of the test due to some unknown distraction. Similar illustration of the voice tests can be found in Figure 3.

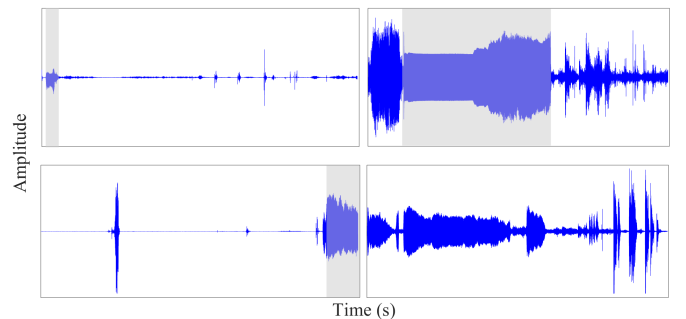


Fig. 3. Illustrative examples of voice clinimetric test sensor data recorded using a smartphone microphone from healthy individuals and those with Parkinson’s disease. The top two tests are performed by healthy individuals and the bottom two by PD patients. Voice tests take approximately 20s and the shaded area marks the part of the test where the user adheres to the test protocol.

TABLE I

Clinimetric test protocols, assumptions and commonly encountered protocol violations in the Smartphone-PD project data used to test the quality control framework proposed in this study.

Test	Protocol	Protocol violations	Hand-labelling protocol
Voice	Place the phone up to your ear as if making a normal phone call. Take a deep breath, and say “aaah” for as long as you can, at a steady volume and pitch.	<ol style="list-style-type: none"> <li>1. User interactions with the smartphone including taking a phone call, texting or playing a game during test.</li> <li>2. User performs test in loud environment.</li> <li>3. Non-sustained vowel phonation activities including coughing, reading out the instructions on the display, talking to another person, during test.</li> </ol>	<ol style="list-style-type: none"> <li>(1) Vowel sound segments are marked as adherence</li> <li>(2) Anything else is marked as non-adherence</li> </ol>
Balance	Place the phone in your pocket. When the buzzer vibrates, stand up straight unaided.	<ol style="list-style-type: none"> <li>1. User interactions with the smartphone including taking a phone call, texting or playing a game during test.</li> <li>2. User is jumping or falling during the test.</li> </ol>	<ol style="list-style-type: none"> <li>(1) Where there is uncertainty in the user’s activity, a non-adherence label is applied</li> <li>(2) Buzzer is labelled as non-adherence</li> <li>(3) Where an interval is confounded with the buzzer, a non-adherence label is given to that interval</li> <li>(4) Where an interval is confounded with an orientation change of the smartphone and the data is otherwise ambiguous, a non-adherence label is given to that interval</li> </ol>
Walking	Stand up and place the phone in your pocket. When the buzzer vibrates, walk forward 20 yards; then turn around and walk back.	<ol style="list-style-type: none"> <li>1. User interactions with the smartphone including taking a phone call, texting or playing a game during test.</li> <li>2. Non-walking activities including jumping, falling or standing still.</li> <li>3. User encounters obstacles during walking which interfere with normal walking.</li> </ol>	<ol style="list-style-type: none"> <li>(1) Where there is uncertainty in the user’s activity, a non-adherence label is applied</li> <li>(2) Buzzer is labelled as non-adherence</li> <li>(3) Where an interval is confounded with the buzzer, a non-adherence label is given to that interval</li> <li>(4) Where an interval is confounded with an orientation change of the smartphone and the data is otherwise ambiguous, a non-adherence label is given to that interval</li> <li>(5) A turn is labelled as adherence</li> </ol>

## V. SENSOR-SPECIFIC PREPROCESSING

Whenever we analyze data from sensors it is often necessary to apply some sensor-specific processing to the raw data to remove various confounds. This is the case for the walking, balance and voice tests described above.

### A. Isolating and removing orientation changes from accelerometry data

One of the primary functions for which MEMs accelerometers were included in smartphones is to detect the orientation in which the user is holding the device and allow for appropriate shift of the display between “landscape” (horizontal) and “portrait” (vertical) display modes. The accelerometer does this by measuring the earth’s gravitational field acting on the smartphone. In recent years there has been an increasing interest in utilizing built-in accelerometer sensors to infer various motion patterns of the user [47]. In clinimetric testing they could be used to assess the ability of the user to perform certain daily activities which can be a strong indicator of a particular health condition. For example, it has been shown that PD can significantly affect activities such as gait or standing upright. In order to use the accelerometer data collected from a smartphone for monitoring gait (or balance), we first need to remove the effect of the earth’s gravitational field from the raw accelerometer data as it is a confounding factor. This is because the accelerometer output is sensitive to the orientation

of the device with respect to the gravitational field, as well as the accelerations due to the user’s motion patterns that we seek to measure.

Let us denote the raw accelerometer output which reflects the total acceleration due to forces applied to the device by  $a_r \in \mathbb{R}^3$ , then we can write:

$$a_r = a_d + a_g \quad (1)$$

where  $a_g \in \mathbb{R}^3$  is the gravitational acceleration acting on the device and  $a_d$  is the sum of the residual accelerations acting on the device (often called “linear” or “dynamic”) acceleration. We are interested in estimating  $a_d$  from  $a_r$  without observing  $a_g$  directly. A widely-used approach involves “sensor fusion” using gyroscopes or other sensors to jointly infer device orientation [48], but this approach relies on access to additional synchronized sensor data. Without additional information we have to make fairly strong assumptions about  $a_g$  and  $a_d$  in order to infer them. A common assumption is that orientation is locally stationary in time, so that passing the raw data through a digital high pass filter of some sort is (under certain mathematical assumptions) the optimal solution. However, this is too restrictive a set of assumptions to make when the user is constantly interacting with the device and performing activity tests at the same time. At the same time it is reasonable to assume that the measured gravitational field will follow relatively simple dynamics compared to the dynamic component. In this work we propose a novel approach which

models the gravitational field as a piecewise linear signal. This assumption is less restrictive than standard stationarity assumptions, but still allows us to rapidly filter away the effect of device orientation.

To estimate the unknown piecewise linear trend  $a_g$  from the raw output  $a_r$ , we use  $L_1$ -trend filtering, which is a variation of the widely-used Hodrick–Prescott (H-P) filter [49]. The  $L_1$ -trend filter substitutes a sum of absolute values (i.e., an  $L_1$  norm) for the sum of squares used in H-P filtering to penalize variations in the estimated trend.

Assume we have  $T$  measurements of the raw accelerometer data ( $T$  data points) and let us denote them by  $x_1, \dots, x_T$  where  $x_t \in \mathbb{R}^3$  for  $t = 1, \dots, T$ . The trend vectors  $g_1, \dots, g_T$  should minimize the objective function:

$$\hat{g} = \arg \min_g \left\{ \frac{1}{2} \sum_{t=1}^T |x_t - g_t| + \lambda \sum_{t=2}^{T-1} |g_{t-1} - 2g_t + g_{t+1}| \right\} \quad (2)$$

where  $\hat{g} = \hat{g}_1, \dots, \hat{g}_T$  denotes the set of gravitational vectors minimizing the functional in (2). The linear acceleration is then estimated by subtracting the estimated gravitational trends from the raw sensor output:  $x_t^d = x_t - \hat{g}_t$  for  $t = 1, \dots, T$ , see Figure 4.

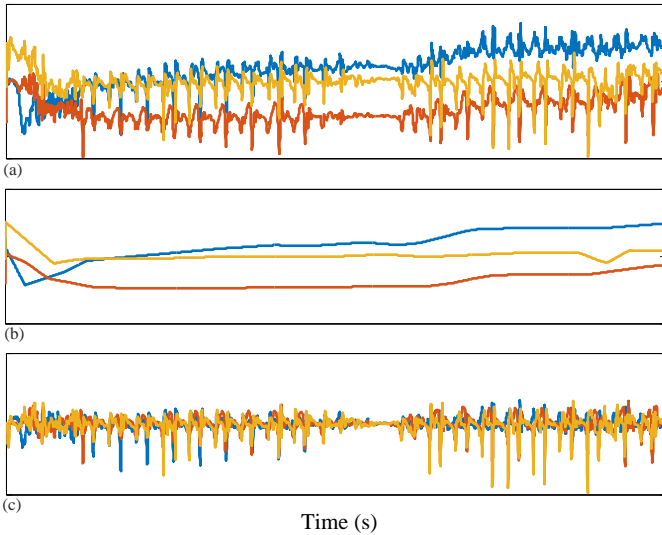


Fig. 4. Raw accelerometer sensor output vector  $x$  for a single walking test (top panel); (a) raw acceleration data, (b) estimated gravitational orientation trend  $\hat{g}$ , (c) estimated dynamic acceleration after removing the effect of device orientation.

### B. Feature extraction

In contrast to existing algorithms for segmentation of sensor data, we propose a simple approach which can use just a single feature for each kind of sensor. The system could be easily extended to include a more sophisticated feature engineering stage, however the benefits of this will depend upon the clinimetric tests analyzed.

We compute the magnitude of the 3-axis dynamic acceleration vector estimated after preprocessing to remove the gravitational orientation component. If we denote the dynamic acceleration at time  $t$  by  $x_t \in \mathbb{R}^3$ , then the magnitude is

the Euclidean norm  $\|x_t\|_2 = \sqrt{x_{t,1}^2 + x_{t,2}^2 + x_{t,3}^2}$ , and this is proportional to the magnitude of the instantaneous dynamic force being applied to the device (the missing constant of proportionality here is the combined, but unknown, mass of the device and the wearer). For quality control of both the walking and balance tests we do not directly model the dynamic acceleration vector, only its magnitude (for the balance tests) and  $\log_{10}$  magnitude (for the walking tests).

In order to efficiently process the data from the voice test we also extract a single feature from the raw sensor output. The raw voice data used in this study is sampled at 44,100 Hz and direct segmentation of this very high-rate signal would be unnecessarily computationally challenging. Instead we segment the original signal into 10ms windows and extract the signal energy of the data in each of those windows which contains 441 unidimensional (and dimensionless) sensor measurements. If we denote the microphone output as  $x_1, \dots, x_T$ , the first window consists of  $\{x_1, \dots, x_{441}\}$ ; the second window  $\{x_{442}, \dots, x_{882}\}$  etc. The signal energy associated with each window is the squared Euclidean norm of the measurements in that frame with the first window denoted by  $\epsilon_1 = \sqrt{\sum_{t=1}^{441} x_t^2}$ .

### C. Downsampling (sample rate reduction)

While we are interested in processing the data at sufficiently high frequency, in some situations modeling the raw directly can be computationally wasteful when our interest is quality control only. We have studied the power spectrum of the different tests to find when we can downsample the original high frequency signal to a lower frequency without losing essential information. In practice appropriate downsampling is particularly important whenever we use AR models. This is because high frequency data requires inferring high number of AR coefficients to accurately capture the dynamics of the data. Estimating large numbers of AR coefficients is difficult because parameter inference in the model requires high computational effort, and since the amount of data is always limited it is also more likely to lead to unreliable estimates for the AR model parameters.

In general, obtaining a representation of a signal which is invariant to downsampling is an ill-posed problem. However, in the special case of *bandlimited* signals it can be shown that ideal reconstruction is possible as long as certain criteria hold. Bandlimited signals have restricted support in the frequency domain such that their Fourier transform is 0 for frequencies  $\omega$  for which  $|\omega| > 2\pi B$  where  $B > 0$  is the *bandwidth* of the signal which reflects the maximum frequency content (Hz). In other words the spectrum of bandlimited signals have support bounded at  $B$ . Given that a signal is bandlimited we can produce an ideal reconstruction of it as long as we have samples from it at a frequency of at least  $2B$ . This minimum sampling frequency requirement which allows for perfect reconstruction is known as the *Nyquist criterion* and specifies that the longest sampling time duration which ensures perfect reconstruction is  $1/(2B)$ . The ideal reconstruction of bandlimited signals from a limited number of samples given that the Nyquist criterion holds can be performed using the

*Shannon-Whittaker reconstruction formula* [50]. If we assume that the high frequency data recorded by the sensors consists of samples from a real signal  $f : \mathbb{R} \rightarrow \mathbb{R}$ , then if  $f$  is bandlimited, according to the Nyquist criterion we can sample the original data at a rate near  $2B$  and reconstruct  $f$  perfectly from the downsampled data.

In the real world most signals are not exactly bandlimited, but their power spectrum shows small magnitude at high frequencies, thus we can apply a low pass filter to the original signal to make it bandlimited. We evaluated the power spectrum of the accelerometer data from each of the 100 walking tests and the 100 balance tests. In Figure 5 we have combined all 100 densities for the walking tests and all 100 densities for the balance tests in the same plot. Figure 5 suggest strong evidence that the  $\log_{10}$  magnitude of the linear acceleration from the walking tests comes from a nearly bandlimited signal with bandlimit  $B < 15\text{Hz}$ . Therefore, after removing the effect of the gravitational component all the data coming from the walking tests is preprocessed with a low-pass filter of a cut-off frequency of 15Hz. Following the Nyquist criterion then we can downsample the signal to uniform sampling rate of  $2 \times 15 = 30\text{Hz}$ .

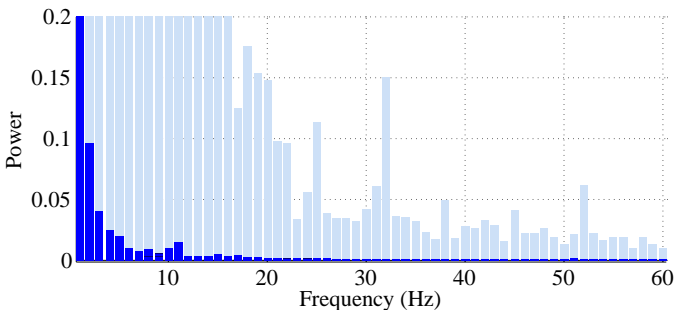


Fig. 5. Power spectra of the magnitude of the 3-axis accelerometer data from each of the 100 balance and walking tests. The 200 densities are plotted on top of each other in order to see the maximum support that was observed at each frequency over all 200 tests. The shaded bars display the power spectra from the balance tests and the colored bars denote the spectra of the walking tests. Since walking is highly periodic, in the spectra of these tests most of the power is found in the lower frequencies associated with periodic walking. During the balance tests periodic activities are observed for very short time durations and the only periodic activity consistently recorded is the smartphone buzzer. This explains why we see that a lot of the power in the spectra is not found at the lower frequencies, but instead spread across the higher frequencies.

There is little evidence (see Figure 5) to support the interpretation that the sensor data for the balance tests is bandlimited, therefore we omit the downsampling step and model the magnitude of the accelerometer data from the balance tests in its original, high sample-rate form.

## VI. SEQUENTIAL BEHAVIOUR MODELLING

It is realistic to assume that for most remote health monitoring technology, detailed user behaviour information would never be available after deployment. Therefore, traditional supervised machine learning activity recognition systems are not applicable and we turn to unsupervised learning. We propose two different methods for segmenting distinct behaviours.

The first method is based on fitting a GMM to the data generated from each clinimetric test. The method does not

require any labeled data for training, but imposes the strong assumption that the data violating the test protocols can be clustered into a different Gaussian component to data which adheres to the protocol. Despite the simplicity of this method, we demonstrate that in some scenarios it manages to segment out most of the bad quality data points with very little computation involved.

For more complex scenarios we also propose a general technique which can be used to segment different behaviours based on the properties of the data into some estimated number of different “states”.

### A. Unsupervised behaviour modeling

One of the primary methodological contributions of this work is obviating the need for elaborate feature engineering. Existing machine learning methods for activity recognition and segmentation of sensor data typically involve windowing the data at the start of the analysis and extracting a rich set of features from each data window with prespecified fixed length (such as 30s, 1min etc.). When it comes to the problem of quality control, in particular for clinimetric data, there are two major problems with this existing approach:

- 1) Any behavior changes which occur in the data within a window cannot be represented (see Figure 6). Due to our inability to model and account for them, they confound the feature values for the window in which they occur. Many of the features used for processing sensor data are some type of frequency domain feature (for example, dominant frequency component; largest magnitude Fourier coefficients; various wavelet coefficients etc.). Frequency domain features are only meaningful for signals that have no abrupt changes; Fourier analysis over windows which contain abrupt discontinuities is dominated by unavoidable Gibb’s phenomena [51]. Unfortunately, behavioural data from clinimetric tests is rife with such discontinuities due to inevitable changes in activities during tests. In the approach we propose, the window sizes and boundaries adapt to the data, since segmentation is learned using a probabilistic model which is specifically designed to capture rapid changes in activity when they occur, but also to model the intricacies of each activity.
- 2) The optimal features to be extracted from each window depend largely on the task/activity occurring in that window. If we are interested in developing a unified framework which works under a realistically wide set of scenarios encountered outside the lab, hand-picking an appropriate set of features for each activity that a clinimetric test might include is not feasible. This issue could be partially overcome if we use “automated” features such as principle component analysis (PCA), but this entails unrealistic assumptions (i.e. linearity). Alternatively, we could use an unsupervised approach for automated feature learning such as layers of restricted Boltzmann machines (RBM) or deep belief networks (DBN). However, these methods require large volumes of data from every behaviour (which is unlikely

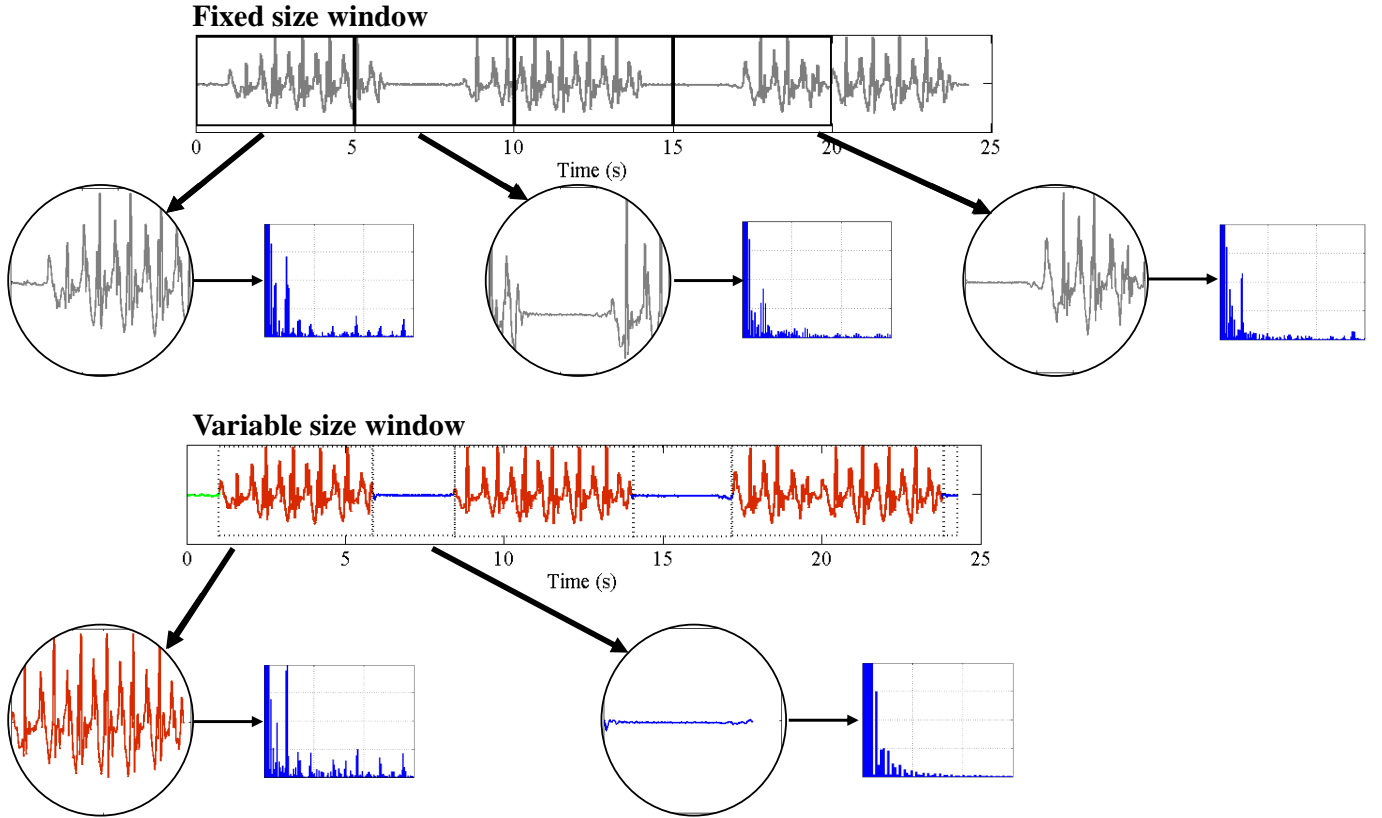


Fig. 6. Demonstration of how the traditional feature extraction approach relying on windowing with fixed window size can lead to misleading estimates of any features from the frequency domain. The bottom plot demonstrates how an accelerometer signal is segmented using a switching AR model and more accurate estimates of frequency domain features can be obtained as a result. We observe this by looking at how the power spectra changes.

to ever be available from health-impaired users), and sufficient computational power to train, making them unsuitable for deployment in real-time applications on smartphones or other resource-constrained devices. Even so, basic RBMs and DBNs would still need to be trained on features extracted after windowing of the sensor data. Additionally, although the features extracted using deep learning systems have demonstrated highly accurate classification results for many applications, we lack any ability to interpret these models to give a human understanding of what aspects of the data they represent. When dealing with healthcare applications, this lack of interpretability could significantly reduce the explanatory power required to gain confidence in the technique. The system we propose does not rely on extensive feature engineering or inscrutable deep learning algorithms, since we demonstrate sufficiently high performance using a single feature for each of the different sensor types. Of course, the proposed approach can be easily extended to use multiple features per data type and this could potentially boost performance when appropriate features are chosen.

*a) Segmentation with GMMs:* The simpler proposal is a GMM-based approach which relies on the assumption that (at least most of the time) the magnitude of the sensor data adhering to the test protocols is different from the magnitude of the data violating them; or that we can approximately cluster

the magnitude of that data into two separate Gaussian components. After we have applied the appropriate pre-processing depending on the data source (as described above) we fit a two-component ( $K = 2$ ) GMM to each of the different sensor datasets. The GMMs are estimated in an unsupervised way using the expectation-maximization (E-M) algorithm where after convergence points are clustered to their most likely component using the maximum-a-posteriori (MAP) principle<sup>1</sup>. Let us denote the preprocessed data by  $x_1, \dots, x_T$  with  $T$  being the number of sensor outputs for a given test after pre-processing. By fitting a  $K = 2$  component GMM to  $x_1, \dots, x_T$  we will estimate some *indicators*  $z_1, \dots, z_T$  which denote the component assignment of each time point (for example  $z_t = 1$  denotes that time point  $x_t$  is associated with component 1). We denote by  $(\mu_1, \sigma_1)$  and  $(\mu_2, \sigma_2)$  the component mean and variance for the first and second component respectively. We use the estimated means  $\mu_1$  and  $\mu_2$  to identify whether the component corresponds to protocol adherence or violation. For walking tests and voice tests we assume that if  $\mu_1 > \mu_2$  all data points  $\{x_t : z_t = 1\}$  represent adherence to the test protocols, hence  $\{x_t : z_t = 2\}$  represent protocol violation. By contrast, for the balance tests we assume that time points associated with the larger mean represent violation and the points associated with the smaller mean

<sup>1</sup>More precisely, each point in time is assigned to the component that maximizes the probability of its component indicator.



represent adherence to the protocols. Since the GMM ignores the sequential nature of the data (see GMM graphical model, Figure 7), the estimated indicators  $z_1, \dots, z_T$  can switch very rapidly between the two components, providing an unrealistic representation of human behaviour. In order to partially address this issue, we apply moving *median filtering* [52] to the indicator  $z_1, \dots, z_T$  and run it repeatedly to convergence. In this way we obtain a “smoothed” sequence  $\hat{u}_1, \dots, \hat{u}_T$  which we use as classification of whether each of  $x_1, \dots, x_T$  is adhering to, or violating, the relevant protocol; time point  $t$  is classified as adherence if  $\hat{u}_t = 1$  and violation if  $\hat{u}_t = 2$ .

b) *Segmentation with the switching AR model*: In order to extend the GMM to model long time-scale dependence in the data we can turn to *hidden Markov models* (HMM) Rabiner [43]. HMMs with Gaussian observations (or mixtures of Gaussian observations) have long dominated areas such as activity [53, 54, 55, 56, 57] and speech recognition [43, 58, 59]. However, simple HMMs fail to model any of the frequency domain features of the data, and are therefore not flexible enough to describe the sensor data; instead we need to use a more appropriate model.

The *switching autoregressive* model is a flexible discrete latent variable model for sequential data which has been widely used in many applications, including econometrics and signal processing [60, 61, 45, 44]. Typically some  $K$  number of different AR models are assumed a-priori. An order  $r$  AR model is a random process which describes a sequence  $x_t$  as a linear combination of previous values in the sequence and a stochastic term:

$$x_t = \sum_{j=1}^r A_j x_{t-j} + e_t \quad e_t \sim \mathcal{N}(0, \sigma^2) \quad (3)$$

where  $A_1, \dots, A_r$  are the AR coefficients and  $e_t$  is a zero mean, Gaussian i.i.d. sequence (we can trivially extend the model such that  $e_t \sim \mathcal{N}(\mu, \sigma^2)$  for any real-valued  $\mu$ ). An important property of AR models is that we can express its *power spectral density* as a function of its coefficients:

$$S(f) = \frac{\sigma^2}{\left|1 - \sum_{j=1}^r A_j \exp(-i2\pi f j)\right|^2} \quad (4)$$

where  $f \in [-\pi, \pi]$  is the frequency variable with  $i$  here denoting the imaginary unit. This means that the order of the AR model directly determines the number of “spikes” in its spectral density, which corresponds to the number of zeros in the numerator of this expression, and therefore the complexity or amount of detail in the power spectrum of  $x_t$  that can be represented.

In switching AR models we assume that the data is an inhomogeneous stochastic process and multiple different AR models are required to represent the dynamic structure of the series, i.e.:

$$x_t = \sum_{j=1}^r A_j^{z_t} x_{t-j} + e_t^{z_t} \quad e_t^{z_t} \sim \mathcal{N}(0, \sigma_{z_t}^2) \quad (5)$$

where  $z_t \in \{1, \dots, K\}$  indicates the AR model associated with point  $t$ . The latent variables  $z_1, \dots, z_T$  describing the

switching process are modeled with a Markov chain. Typically,  $K \ll T$  allowing us to cluster together data which is likely to be modeled with the same AR coefficients.

The switching AR model above is closely related to the HMM: as with the switching AR model, the HMM also assumes that data is associated with a sequence of hidden (latent) variables which follow a Markov process ( $z_1, \dots, z_T$  in Figure 7). However, in the case of HMMs we assume that given the latent variables the observed data is independent. In other words, the simplest HMM can be considered as a switching AR model where the order  $r$  of each AR is 0 with non-zero mean error term. Neither of the models discussed here are necessarily limited to Gaussian data and there have been HMM extensions utilizing: multinomial states for part-of-speech tagging [62], Laplace distributed states for passive infrared signals [57] or even neural network observational models for image and video processing [63].

The segmentation produced with any variant of the HMM is highly dependent on the choice of  $K$  (the number of hidden Markov states i.e. distinct AR models). In the problem we study here, the number  $K$  would roughly correspond to the number of different behavioural patterns which occur during each of the clinimetric tests. However, it is not realistic to assume we can anticipate how many different behaviours can occur during each test. In fact it is likely that as we collect data from more tests, new patterns will emerge and  $K$  will need to change. This motivates us to seek a *Bayesian nonparametric* (BNP) approach to this segmentation problem: a BNP extension of the switching AR model described above which will be able to accommodate an unknown and changing number  $K^+$  of AR models.

The nonparametric switching AR model (first derived as a special case of nonparametric switching linear dynamical systems in Fox et al. [64]) is obtained by augmenting the transition matrix of the HMM underlying the switching AR with a *hierarchical Dirichlet process* (HDP)[65] prior (see Figure 7). Effectively, the HMM component of the switching AR model is replaced with an *infinite* HMM [66]. The infinite HMM avoids fixing the number of states  $K$  in the Markov model; instead it assumes that the number of HMM states an unknown, and potentially large  $K^+$ , and depends upon the amount of training data we have already seen. Whenever we are fitting an infinite HMM we typically start by assigning the data into a single hidden state (or a small fixed number of states) and at each step with some probability we increase the number of effective states at each inference pass through the signal. In this way it is possible to infer the number of effective states in an infinite HMM as a random variable from the data. The parameters specifying how quickly the number of effective states grows are called *local* and *global concentration* hyperparameters:  $\alpha$  denotes the local and  $\gamma$  the global concentration.

The local  $\alpha$  controls how likely it is that new types of transitions occur between the effective states, or essentially how sparse is the HMM transition matrix. The global  $\gamma$  reflects how likely is it for a new effective state to arise, or how many rows the transition matrix has. Unlike the fixed  $K$  in standard parametric HMMs, the hyperparameters  $\alpha$  and  $\gamma$  of

the infinite HMM (or any of its extensions) can be tuned with standard model selection tools which compute how the value of the *complete data likelihood* changes as  $\alpha$  and  $\gamma$  change. This allows us to model the behavioural patterns in the smartphone clinimetric tests in a completely unsupervised way. For a lengthier discussion and derivation of the infinite HMM and the nonparametric switching AR model, we refer readers to [66, 65, 64].

As Fox et al. [64] remarks, the switching AR model can be also be obtained as a special case of a more general switching linear dynamical systems (LDS) model [67]. In the LDS we assume that the observations are noisy measurements of the quantity of interest. The switching LDS allows for even more flexible segmentation analysis of the different behavioural states, but this comes at the cost of substantial increase in model complexity. Additional analysis showed that for the chosen data, the most parsimonious solution is offered by the switching AR.

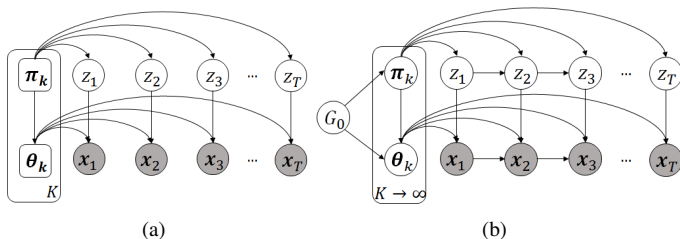


Fig. 7. Probabilistic graphical models for (a) Gaussian mixture model (GMM) and (b) nonparametric switching autoregressive (AR) model. The GMM component parameters  $\theta_k$  are the mean and the variance of data associated with component  $k$ . By contrast, the component parameters  $\theta_k$  for the switching AR consist of the AR coefficients  $A_1^k, \dots, A_r^k$  and the AR error parameters  $\mu_k$  and  $\sigma_k$ . Parameter  $\pi_k$  denotes the mixing coefficients and the transition matrix for the GMM and the switching AR, respectively. In the parametric GMM  $\pi_k$  and  $\theta_k$  are fixed. In the nonparametric switching AR  $\pi_k$  and  $\theta_k$  are modeled with an HDP prior, where  $G = \{G_1, \dots, G_{K^+}\} \sim \text{HDP}(\alpha, \gamma, \theta_0)$ . Hyperparameter  $\theta_0$  denotes the conjugate prior over the  $A^k$ 's, the  $\mu^k$ 's and the  $\sigma^k$ 's. See main text for further description of the HDP and its concentration parameters  $\alpha$  and  $\gamma$ .

### B. Segmentation context mapping

The switching AR model groups together intervals of the preprocessed data that have similar dynamics described by the same AR pattern, i.e. we group points  $x_t$  according to their corresponding indicator values  $z_t = k$  for  $k \in \{1, \dots, K^+\}$ . The generality of this principle allows us to apply the framework widely across different data sets generated from diverse clinimetric tests such as walking, balance or voice tests.

A trained expert can reasonably identify intervals of walking or balancing that adhere to the corresponding test protocols, while specific physical activities would be difficult to identify purely from the accelerometer output. Lack of behaviour labels can challenge our understanding of the segmentation from the previous stage. This motivated the collection of additional controlled clinimetric tests to shed some light on the patterns we discover using the nonparametric switching AR model. The controlled smartphone tests have been performed by healthy controls. We collect 32 walking, 32 balance and 32 voice tests in which we vary the orientation and location of the

phone during a simulated clinimetric test. During these tests the participants are instructed to perform some of the most common behaviours which we observe during clinimetric tests performed outside the lab. Activities conducted during the tests include, freezing of gait, walking, coughing, sustained phonation, keeping balance, and several others. A human expert annotates the monitored behaviours with  $b_1, \dots, b_T$  which associate each data point with a behavioural label (i.e.  $b_t = \text{“walking”}$  means point  $x_t$  was recorded during walking). By contrast to the clinimetric tests performed outside the lab, here we have relatively detailed information about what physical behaviour was recorded in each segment of these controlled tests.

Since we have the “ground truth” labels  $b$  for the controlled clinimetric tests, we can be confident in the interpretation of the intervals estimated by the unsupervised learning approach. This allows us to better understand the different intervals inferred from data collected from outside the lab, when labels  $b$  are not available. Note that  $b_1, \dots, b_T$  are not used during the training of the nonparametric switching AR model, but only for validation. Furthermore, the distribution of the data from the actual clinimetric tests collected outside of the lab significantly departs from the distribution of the data of the controlled tests.

We assess the ability of the model to segment data consisting of different behaviours. This is done by associating each of the unique  $K^+$  values that the indicators  $z$  can take with one of the behavioural labels occurring during a controlled test. For each  $k \in \{1, \dots, K^+\}$ , state  $k$  is assumed to model behaviour  $b_k$  with  $b_k = \text{mode}\{b_t : z_t = k\}$  being the most probable behaviour during that state.

Using this simple mapping from the numerical indicators  $z_1, \dots, z_T$  to interpretable behaviours, we obtain estimated behaviour indicators  $\hat{z}_1, \dots, \hat{z}_T$ . Using the estimated behaviour indicators  $\hat{z}_1, \dots, \hat{z}_T$  and the “ground truth” labels  $b_1, \dots, b_T$  we compute the following algorithm performance measures: balanced accuracy (BA), true positive (TP) and true negative (TN) rates for the segmentation approach in Table II. For example given behaviour  $b^*$ , these metrics are computed using:

$$\text{TP} = \frac{\sum_{t=1}^T \mathbf{1}(\hat{z}_t = b^* \cap b_t = b^*)}{\sum_{t=1}^T \mathbf{1}(\hat{z}_t = b^*)}; \text{TN} = \frac{\sum_{t=1}^T \mathbf{1}(\hat{z}_t \neq b^* \cap b_t \neq b^*)}{\sum_{t=1}^T \mathbf{1}(\hat{z}_t \neq b^*)},$$

$$\text{BA} = \frac{\text{TP} + \text{TN}}{2} \quad (6)$$

where  $\mathbf{1}(\cdot)$  denotes the indicator function which is 1 if the logical condition is true, zero otherwise.

Outside the lab we cannot always label physical behaviours with high confidence. Instead, we use binary labels  $u_1, \dots, u_T$  which take values  $u_t = 1$  if point  $x_t$  adheres or  $u_t = 2$  if it violates the applicable test protocol (as described in Section IV-B). In order to classify a time point  $x_t$  with respect to its adherence to the protocol, it is sufficient to simply classify the state assignment  $z_t$  associated with that time point.

To automate this context mapping, we use a very highly interpretable *naive Bayes classifier*. We train the classifier

TABLE II

Balanced accuracy (BA), true positive (TP) and true negative (TN) rates for the nonparametric switching AR model trained on walking and balance tests performed in a controlled environment. The TP rate reflects the ability to correctly identify an activity when occurring and the TN rate reflects the ability to correctly indicate lack of that activity whenever not occurring.

Behaviour	BA	TP	TN
Walking	95%	96%	93%
Standing up straight	95%	98%	91%
Phone stationary	98%	100%	95%
Sustained phonation	98%	99%	97%

using the posterior probabilities<sup>2</sup> of the indicators  $z_1, \dots, z_T$  associated with the training data as inputs and the corresponding binary labels  $u_1, \dots, u_T$  as outputs. For a new test point  $\tilde{x}$  we can then compute the vector of probabilities  $P(\tilde{z} | x_1, \dots, x_T, \theta, \pi)$  given the switching AR parameters  $\theta$  and  $\pi$  (explained in Figure 7) and rescale them appropriately to appear as integer frequencies; we will write those vectors of frequencies as  $p_{\tilde{z}} = (p_{\tilde{z},1}, \dots, p_{\tilde{z},K^+})$ . The naive Bayes classifier assumes the following probabilistic model:

$$P(p_{\tilde{z}} | u_1, \dots, u_T, \tilde{u}, p_{z_1}, \dots, p_{z_T}) = \frac{(\sum_{k=1}^{K^+} p_k)!}{\prod_{k=1}^{K^+} p_k!} \prod_{k=1}^{K^+} \bar{\pi}_{k,\tilde{u}}^{p_k} \quad (7)$$

where  $\bar{\pi}_{k,\tilde{u}}$  denotes the training probability for attribute  $k$  given observation is from class  $\tilde{u}$ . This model can be then reversed (via Bayes rule) to predict the class assignment  $\hat{u} \in \{1, 2\}$ , for some unlabeled input  $p_{\tilde{z}}$ :

$$\hat{u} = \arg \max_{c \in \{1,2\}} \left[ \log P(\tilde{u} = c) + \sum_{k=1}^{K^+} p_k \log(\bar{\pi}_{k,c}) \right] \quad (8)$$

with  $P(\tilde{p} = c)$  enabling control over the prior probabilities for class adherence/violation of the protocols.

The multinomial naive Bayes is linear in the log-space of the input variables, making it very easy to understand; we demonstrate this by plotting a projection of the input variables and the decision boundary in 2-D (Figure 8). The naive Bayes classifier requires very little training data to estimate parameters, scales linearly with the data size, and despite its simplicity has shown performance close to state of the art for demanding applications such as topic modeling in natural language processing, spam detection in electronic communications and others [68]. One of the main disadvantages of this classifier is that it assumes, usually unrealistically, that the input variables are independent, however this is not an issue in this application since the classifier is trained on a single feature. The multinomial naive Bayes classifier assumes that data in the different classification classes follow different multinomial distributions (Figure 9).

For different clinimetric tests, we need to train different classifiers because when the test protocols change so does the association between the  $z$ 's and the  $u$ 's. However, the overall framework we use remains universal across the different tests

<sup>2</sup>We noticed that we can obtain very similar accuracy using just the modal estimates of the indicators  $z_1, \dots, z_T$  as an input to the classifier, which takes substantially less computational effort compared to computing the full posterior distribution of the indicators.

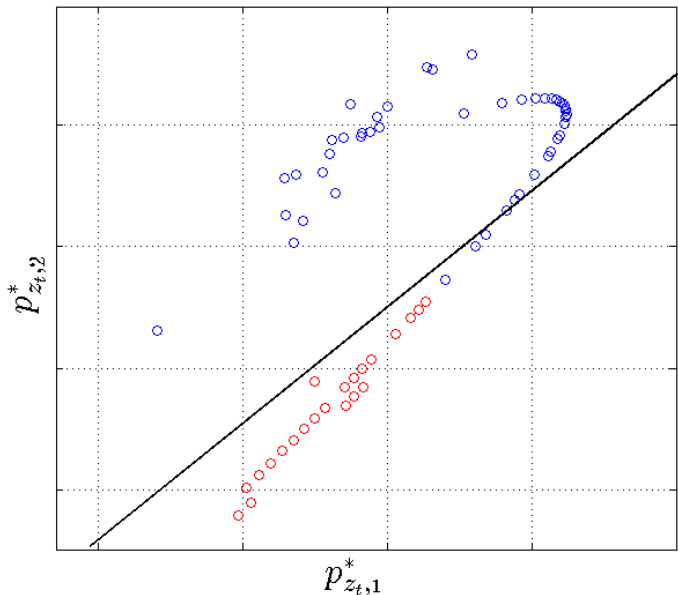


Fig. 8. Visualizing the context mapping of behavioural segmentation to clinimetric protocol adhere/violation predictions, data from a single walking test. The log of the input segmentation state probabilities  $p_{z_1}, \dots, p_{z_T}$  is projected into 2-D using linear discriminant analysis (LDA), projections are denoted with  $p_{z_t}^*$  where the  $p_{z_t}$  is a  $K^+$  dimensional vector and  $p_{z_t}^*$  is 2-D. Input projections are labeled with adherence (red) and violation (blue). The “linear” structure can be explained with the fact that typically, a data point  $x_t$  is associated with high probability to only 1 of  $K^+$  AR states in the behavioural segmentation (and low probability for the remaining AR states) so that the input vector  $p_{z_t}$  is sparse. The decision boundary of the multinomial naive Bayes classifier is also projected (using the same LDA coefficients) onto 2-D (black line). A few outlier projections  $p_{z_t}^*$  are outside the plot axis limits, but they do not affect significantly the decision boundary and yet reduce the visual interpretability of the projection of the bulk of the data.

and can be extrapolated to handle quality control in a wide set of clinimetric testing scenarios.

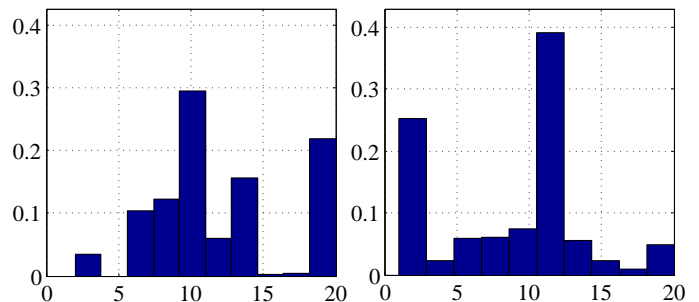


Fig. 9. Normalized histograms of the state variable values associated with data labeled as adherence (left) and non-adherence (right) to the walking test protocol.

## VII. EVALUATION

In order to evaluate the performance of the proposed framework, data from 300 clinimetric tests (100 walking, 100 balance and 100 voice tests) performed by PD patients and healthy controls from the Smartphone-PD study (see Abiola et al. [69]) was processed using the steps described above. The accelerometer data from the walking and balance tests is recorded at frequency rates varying between 50Hz and

200Hz. It is interpolated to a uniform rate of 120Hz (using standard cubic spline interpolation) and the orientation is removed using  $L_1$ -trend filtering as described in Section V-A. We extract the log-amplitude of the dynamic acceleration component for the walking tests and the amplitude of the dynamic component for the balance tests which serve as input to the behavioural segmentation step. The log-amplitude for the walking tests is also down-sampled by factor 4 resulting in a length of  $\sim 90,000$  one-dimensional sequential preprocessed time series; balance tests are not down-sampled giving a length of  $\sim 241,000$  one-dimensional time series. For the voice tests, the extracted energy of each 10 ms frame consists of a length of  $\sim 200,000$  one-dimensional energy time series.

First, the 2-component GMM-based approach described above is evaluated for each of the three data sets where performance is reported in Table III. The metrics are estimated using the expressions (6) where we compare the estimated binary indicators  $\hat{u}_1, \dots, \hat{u}_T$  and “ground truth” labels  $u_1, \dots, u_T$  denoting adherence/violation. Since this approach is completely unsupervised, we use all the data for training, but none of the labels are used for validation. While the GMM is not flexible enough to model the full composite behavioural complexity of the data captured during most clinimetric tests, we observe high accuracies for the voice tests. This is because the protocol for voice tests consist only of producing sustained vocal phonations in very close proximity to the sensor. Therefore, it can be argued that adherence to the protocol for this activity is distinguishable based on an appropriate measure of magnitude of the sensor recordings alone, largely ignoring the longer-scale temporal variations. In tests where the protocol requires the user to perform behaviours with more complex, composite dynamics, the limitations of the simple GMM become more apparent. For example, this occurs during the walking tests where protocol violations can be distinguished a lot more accurately if the behavioural segmentation model also incorporates both the longer-term sequential nature of the data and its spectral information.

Next, the nonparametric switching AR behavioural segmentation model is fitted to each of the three data sets where we specify the maximum order of the AR models associated with each state to  $r = 4$ . For the evaluation here parameter inference is performed using the truncated block Gibbs sampler described in Fox et al. [64]. For future, real-time deployment we can use more scalable deterministic algorithms based on extensions of Hughes et al. [70] and Raykov et al. [71].

As described above, we now input the state indicators  $z_1, \dots, z_T$  to a multinomial, naive Bayes classifier where if an indicator value has not been seen during training, we assume it is classified as a violation of the protocol during testing. The ability of the method to correctly classify adherence and violations to the protocols of the three tests is measured using standard 10-fold cross validation. The mean and standard deviation of the BA, TP and TN rates of the classifier are shown in Table III. Note that in contrast to Section (VI-B) the accuracy metrics are now comparing the binary labels  $u$  and estimated  $\hat{u}$ . Both the TP and TN values are consistently high across all tests, but the fact that the TN values are close to

TABLE III

Performance of the two proposed algorithms for quality control of clinimetric data and comparison with randomized classifier. For the naive Bayes and the randomized classifiers quality control predictions over all time points are evaluated using 10-fold cross validation. We report mean and standard deviation (in the brackets) of the balanced accuracy (BA), true positive (TP) and true negative (TN) rates across the different cross validation trials changing the subsets of data used for training and testing. For the GMM-based approach we report the BA, TP and TN rates using all the data for training and for testing since this approach is completely unsupervised; standard deviation is not meaningful for a single trial (hence standard deviations are omitted).

	Walking tests	Balance tests	Voice tests
Naive Bayes + nonparametric switching AR			
BA	85% (11%)	81% (14%)	89% (8%)
TP	85% (18%)	81% (16%)	88% (9%)
TN	90% (8%)	88% (9%)	91% (9%)
GMM + running median filtering			
BA	62%	24%	99%
TP	80%	74%	86%
TN	89%	82%	96%
Randomized classifier			
BA	50% (1%)	50% (0.2%)	53% (24%)
TP	1% (0.4%)	0.4% (0.02%)	99% (1%)
TN	100%	100%	6% (23%)

90% for all three tests suggests a low probability of incorrectly labeling data that adheres to the test protocol as a violation of the protocol. In practice, the confidence in this prediction of adherence/violation of protocol can be assessed using the state assignment probabilities in the naive Bayes classifier associated with each time series data point<sup>3</sup>.

In order to ensure that the reported classification accuracy is due to the meaningful segmentation produced by the nonparametric switching AR, we also report the performance of a multinomial naive Bayes classifier (Table III) trained on the shuffled state indicators estimated via the nonparametric switching AR during the segmentation stage. In this way, the classifier is trained on identical data but with randomized association between the data and the training labels (i.e.  $\{z_1, \dots, z_T\}$  are randomly permuted while keeping  $\{u_1, \dots, u_T\}$  fixed). If the association between estimated state indicators and training labels is an accurate representation we would expect a classifier trained on the shuffled indicators to score balanced accuracy of around 50%.

## VIII. FUTURE WORK

### A. Simultaneous multiple sensors

The proposed framework is not limited to specific types of clinimetric activity tests nor specific sensors. It was demonstrated that it can be applied to voice and accelerometer data from three different smartphone clinimetric tests, but the approach could be easily generalized to different sensor-generated time series. For example, it would be straightforward to preprocess multiple sensor types obtained simultaneously during a test and then model these combined sensors together to perform segmentation. This may increase the accuracy of quality control.

<sup>3</sup>The state assignment probabilities for each class of the naive Bayes are the terms inside the  $\arg \max$  operator in (7) after normalization.

### B. Practical, real-time deployment

Mobile, sensor-based applications that can support research into the detection and symptom monitoring of PD have already been deployed on a large scale outside the lab. The iPhone-based mPower app and associated study has enrolled over 10,000 study participants since 2015. Incorporating the proposed system into PD research apps such as mPower could provide automatic, real-time quality control of the smartphone clinimetric tests. This could automatically remove any data which violates the test protocol, eliminating the need to store, transfer or analyze unwanted data. Alternatively, data assessment in real-time on board the data collection device could notify participants to re-do a given clinimetric test to ensure that sufficient amounts of useful, high quality data can be reliably collected.

The most computationally demanding component of the proposed system is the inference of the nonparametric switching AR model. However, the switching AR model can be seen as an extension of the infinite HMM. Therefore in order to perform real-time inference of the model on smartphone or wearable devices, we can use the computational optimization proposed in Raykov et al. [57] and Leech et al. [72] which enables inference of an infinite HMM on a highly resource-constrained microcontroller computing device.

### C. Contextual learning

“Passive monitoring”, where sensor data is captured in an entirely ambulatory way under realistic conditions outside the lab, provides a way to study PD symptoms objectively without interrupting routine activities. The successful monitoring of such daily behavioural details may provide unprecedented insight into the objective monitoring of individuals living with PD. However, outside the lab we usually have little information about the routine activities under measurement unless other, simultaneous monitoring methods are used, such as video recording. However, video monitoring of patients in their homes is expensive and can impact the integrity of the data as it is highly invasive; patient behaviour may be altered under the awareness of video monitoring. In addition, without multiple cameras in each room, it is not possible to follow patients at different locations which means that videoing every daily activity a patient performs is impractical. The system proposed here can be trained to recognize specific patient activities and help researchers identify segments of the passive monitoring data which are most relevant for subsequent analysis. For example, consider patients being passively monitored using smartphones, where researchers wish to assess the effect of some medication on symptoms such as slowness of movement [73] or postural sway [7]. With very few labelled instances of the relevant behaviours, the system proposed here can learn to identify gait and balance behaviours from the continuous, passive sensor data which will assist the researchers into objectively testing their hypothesis.

## IX. CONCLUSION

This report describes a unified algorithm framework for quality control segmentation of clinimetric tests utilizing sensing technologies to remotely monitor patient health outside the

lab. Monitoring patients in their natural environment allows for a more realistic and accurate assessment of an individual’s health, improves accuracy of outcomes in clinical trials in response to therapy and reduces hospital stay [74]. Nonetheless, the unknown nature of the conditions under which data is collected in this way raises suspicions about the quality of the data and its interpretability. Thus, creating a systematic, automated algorithmic approach which analyses the quality of the data could lead to smartphones and wearable devices taking a central role as tools for scientific data collection and monitoring.

This report uses a semi-supervised, nonparametric switching AR model combined with a simple classifier to extract segments of smartphone sensor data that adhere to the assumptions of the appropriate clinimetric test protocol. The feasibility of this approach was demonstrated by applying it to different smartphone clinimetric tests and sensor data types, achieving segmentation accuracies of up to 90% at the resolution of the downsampled data.

By extracting segments of the sensor data that adhere to the assumptions of a test protocol, it is possible to strip the data of confounding factors in the environment that may threaten reproducibility and replicability.

## ACKNOWLEDGMENT

This work was partially supported by the Michael J. Fox Foundation [Grant ID: 10824], UCB Pharma, and in part by a research grant from the NIH (P20 NS92529). The authors gratefully acknowledge Andong Zhan for developing the smartphone application used in this study. The authors express their sincere gratitude to every individual who participated in this study to generate the data used here.

## REFERENCES

- [1] J. Dai, X. Bai, Z. Yang, Z. Shen, and D. Xuan. PerFallID: A pervasive fall detection system using mobile phones. In *2010 8th IEEE International Conference on Pervasive Computing and Communications Workshops (PERCOM Workshops)*, pages 292–297, 2010.
- [2] K. Sha, G. Zhan, W. Shi, M. Lumley, C. Wiholm, and B. Arnetz. SPA: a smart phone assisted chronic illness self-management system with participatory sensing. In *Proceedings of the 2nd International Workshop on Systems and Networking Support for Health Care and Assisted Living Environments*, pages 5:1–5:3, 2008.
- [3] N. Oliver and F. Flores-Mangas. HealthGear: Automatic sleep apnea detection and monitoring with a mobile phone. *Journal of Communications*, 2(2):1–9, 2007.
- [4] N. Maisonneuve, M. Stevens, M. E. Niessen, and L. Steels. Noisetube: Measuring and mapping noise pollution with mobile phones. In *Information Technologies in Environmental Engineering: Proceedings of the 4th International ICSC Symposium Thessaloniki*, pages 215–228, 2009.
- [5] M. Mun, S. Reddy, K. Shilton, N. Yau, J. Burke, D. Estrin, M. Hansen, E. Howard, R. West, and P. Boda. PEIR, the personal environmental impact report, as a

- platform for participatory sensing systems research. In *Proceedings of the 7th International Conference on Mobile Systems, Applications, and Services*, pages 55–68, 2009.
- [6] A. Thiagarajan, L. Ravindranath, K. LaCurts, S. Madden, H. Balakrishnan, S. Toledo, and J. Eriksson. VTrack: accurate, energy-aware road traffic delay estimation using mobile phones. In *Proceedings of the 7th ACM Conference on Embedded Networked Sensor Systems*, pages 85–98, 2009.
- [7] S. Arora, V. Venkataraman, S. Donohue, K. M. Biglan, E. R. Dorsey, and M. A. Little. High accuracy discrimination of Parkinson’s disease participants from healthy controls using smartphones. In *2014 IEEE International Conference on Acoustics, Speech and Signal Processing (ICASSP)*, pages 3641–3644, 2014.
- [8] R. A. Joundi, J.-S. Brittain, N. Jenkinson, A. L. Green, and T. Aziz. Rapid tremor frequency assessment with the iPhone accelerometer. *Parkinsonism & Related Disorders*, 17(4):288–290, 2011.
- [9] N. Kostikis, D. Hristu-Varsakelis, M. Arnaoutoglou, and C. Kotsavasiloglou. Smartphone-based evaluation of parkinsonian hand tremor: Quantitative measurements vs clinical assessment scores. In *2014 36th Annual International Conference of the IEEE Engineering in Medicine and Biology Society*, pages 906–909, 2014.
- [10] K. L. Andrzejewski, A. V. Dowling, D. Stamler, T. J. Felong, D. A. Harris, C. Wong, H. Cai, R. Reilmann, M. A. Little, J. Gwin, K. M. Biglan, and E. R. Dorsey. Wearable sensors in Huntington disease: a pilot study. *Journal of Huntington’s Disease*, 5(2):199–206, 2016.
- [11] G. Rigas, A. T. Tzallas, M. G. Tsiouras, P. Bougia, E. E. Tripoliti, D. Baga, D. I. Fotiadis, S. G. Tsouli, and S. Konitsiotis. Assessment of tremor activity in the Parkinson’s disease using a set of wearable sensors. *IEEE Transactions on Information Technology in Biomedicine*, 16(3):478–487, 2012.
- [12] S. Patel, K. Lorincz, R. Hughes, N. Huggins, J. Growdon, D. Standaert, M. Akay, J. Dy, M. Welsh, and P. Bonato. Monitoring motor fluctuations in patients with Parkinson’s disease using wearable sensors. *IEEE Transactions on Information Technology in Biomedicine*, 13(6):864–873, 2009.
- [13] W. Maetzler, J. Domingos, K. Srulijes, J. J. Ferreira, and B. R. Bloem. Quantitative wearable sensors for objective assessment of Parkinson’s disease. *Movement Disorders*, 28(12):1628–1637, 2013.
- [14] J. Fan, F. Han, and H. Liu. Challenges of big data analysis. *National Science Review*, 1(2):293–314, 2014.
- [15] A. Bulling, U. Blanke, and B. Schiele. A tutorial on human activity recognition using body-worn inertial sensors. *ACM Computer Surveys*, 46(3):33:1–33:33, 2014.
- [16] R. Zhang, Z. Peng, L. Wu, B. Yao, and Y. Guan. Fault diagnosis from raw sensor data using deep neural networks considering temporal coherence. *Sensors*, 17(3):549, 2017.
- [17] A. Börve, J. D Gyllencreutz, K. Terstappen, E. J Backman, A. Alden-Bratt, M. Danielsson, M. Gillstedt, C. Sandberg, and J. Paoli. Smartphone teledermoscopy referrals: a novel process for improved triage of skin cancer patients. *Acta Dermato-Venereologica*, 95(2):186–190, 2015.
- [18] R. D. Stedtfeld, D. M. Tourlousse, G. Seyrig, T. M. Stedtfeld, M. Kronlein, S. Price, F. Ahmad, E. Gulari, J. M. Tiedje, and S. A. Hashsham. Gene-Z: A device for point of care genetic testing using a smartphone. *Lab on a Chip*, 12(8):1454–1462, 2012.
- [19] B. Odeh, R. Kayyali, S. Nabhani-Gebara, and N. Philip. Optimizing cancer care through mobile health. *Supportive Care in Cancer*, 23(7):2183–2188, 2015.
- [20] D. J. Hand. Classifier technology and the illusion of progress. *Statistical Science*, 21(1):1–14, 2006.
- [21] M.-Z. Poh, T. Loddenkemper, C. Reinsberger, N. C. Swenson, S. Goyal, M. C. Sabtala, J. R. Madsen, and R. W. Picard. Convulsive seizure detection using a wrist-worn electrodermal activity and accelerometry biosensor. *Epilepsia*, 53(5):93–97, 2012.
- [22] F. Lipsmeier, I. Fernandez Garcia, D. Wolf, T. Kilchenmann, A. Scotland, J. Schjodt-Eriksen, W.-Y. Cheng, J. Siebourg-Polster, L. Jin, J. Soto, L. Verselis, M. Martin Facklam, F. Boess, M. Koller, M. Grundman, M. A. Little, A. Monsch, R. Postuma, A. Gosh, T. Kremer, K. Taylor, C. Czech, C. Gossens, and M. Lindemann. Successful passive monitoring of early-stage Parkinson’s disease patient mobility in Phase I RG7935/PRX002 clinical trial with smartphone sensors. *Movement Disorders*, 32(2), 2017.
- [23] S. R. Edgar, T. Swyka, G. Fulk, and E. S. Sazonov. Wearable shoe-based device for rehabilitation of stroke patients. In *2010 Annual International Conference of the IEEE Engineering in Medicine and Biology*, pages 3772–3775, 2010.
- [24] G. Charpentier, P.-Y. Benhamou, D. Dardari, A. Clergeot, S. Franc, P. Schaepelynck-Belicar, B. Catargi, V. Melki, L. Chaillous, A. Farret, J.-L. Bosson, A. Penfornis, and on behalf of the TeleDiab Study Group. The Diabeo software enabling individualized insulin dose adjustments combined with telemedicine support improves HbA<sub>1c</sub> in poorly controlled type 1 diabetic patients. *Diabetes Care*, 34(3):533–539, 2011.
- [25] E. Ozdalga, A. Ozdalga, and N. Ahuja. The smartphone in medicine: A review of current and potential use among physicians and students. *Journal of Medical Internet Research*, 14(5):128, 2012.
- [26] A. S. M. Mosa, I. Yoo, and L. Sheets. A systematic review of healthcare applications for smartphones. *BMC Medical Informatics and Decision Making*, 12(1):67, 2012.
- [27] K. J. Kubota, J. A. Chen, and M. A. Little. Machine learning for large-scale wearable sensor data in Parkinson’s disease: Concepts, promises, pitfalls, and futures. *Movement Disorders*, 31(9):1314–1326, 2016.
- [28] I. García-Magariño, C. Medrano, I. Plaza, and B. Oliván. A smartphone-based system for detecting hand tremors in unconstrained environments. *Personal and Ubiquitous Computing*, 20(6):959–971, 2016.

- [29] N. Y. Hammerla, J. Fisher, P. Andras, L. Rochester, R. Walker, and T. Plötz. PD disease state assessment in naturalistic environments using deep learning. In *Proceedings of the Twenty-Ninth AAAI Conference on Artificial Intelligence*, pages 1742–1748, 2015.
- [30] J. Reimer, M. Grabowski, O. Lindvall, and P. Hagell. Use and interpretation of on/off diaries in Parkinson’s disease. *Journal of Neurology, Neurosurgery & Psychiatry*, 75(3): 396–400, 2004.
- [31] J. Hoff, A. van den Plas, E. Wagemans, and J. van Hilten. Accelerometric assessment of levodopa-induced dyskinesias in Parkinson’s disease. *Movement Disorders*, 16(1):58–61, 2001.
- [32] B. T. Cole, S. H. Roy, C. J. D. Luca, and S. H. Nawab. Dynamic neural network detection of tremor and dyskinesia from wearable sensor data. In *2010 Annual International Conference of the IEEE Engineering in Medicine and Biology*, pages 6062–6065, 2010.
- [33] J. P. Giuffrida, D. E. Riley, B. N. Maddux, and D. A. Heldman. Clinically deployable Kinesia<sup>TM</sup> technology for automated tremor assessment. *Movement Disorders*, 24(5):723–730, 2009.
- [34] D. G. Zwartjes, T. Heida, J. P. Van Vugt, J. A. Geelen, and P. H. Veltink. Ambulatory monitoring of activities and motor symptoms in Parkinson’s disease. *IEEE Transactions on Biomedical Engineering*, 57(11):2778–2786, 2010.
- [35] A. Salarian, H. Russmann, F. J. Vingerhoets, P. R. Burkhard, and K. Aminian. Ambulatory monitoring of physical activities in patients with Parkinson’s disease. *IEEE Transactions on Biomedical Engineering*, 54(12): 2296–2299, 2007.
- [36] A. T. Tzallas, M. G. Tsipouras, G. Rigas, D. G. Tsilikakis, E. C. Karvounis, M. Chondrogiorgi, F. Psomadellis, J. Cancela, M. Pastorino, M. T. A. Waldmeyer, S. Konitsiotis, and D. I. Fotiadis. PERFORM: A system for monitoring, assessment and management of patients with Parkinson’s disease. *Sensors*, 14(11):21329–21357, 2014.
- [37] T. Guo, Z. Yan, and K. Aberer. An adaptive approach for online segmentation of multi-dimensional mobile data. In *Proceedings of the Eleventh ACM International Workshop on Data Engineering for Wireless and Mobile Access*, pages 7–14, 2012.
- [38] L. Zelnik-Manor and M. Irani. Statistical analysis of dynamic actions. *IEEE Transactions on Pattern Analysis and Machine Intelligence*, 28(9):1530–1535, 2006.
- [39] C. Lu and N. J. Ferrier. Repetitive motion analysis: segmentation and event classification. *IEEE Transactions on Pattern Analysis and Machine Intelligence*, 26(2): 258–263, 2004.
- [40] F. Zhou, F. De la Torre, and J. K. Hodgins. Hierarchical aligned cluster analysis for temporal clustering of human motion. *IEEE Transactions on Pattern Analysis and Machine Intelligence*, 35(3):582–596, 2013.
- [41] E. Keogh, S. Chu, D. Hart, and M. Pazzani. An online algorithm for segmenting time series. In *Proceedings 2001 IEEE International Conference on Data Mining*, pages 289–296, 2001.
- [42] R. V. Shannon, F.-G. Zeng, V. Kamath, J. Wygonski, and M. Ekelid. Speech recognition with primarily temporal cues. *Science*, 270(5234):303–304, 1995.
- [43] L. R. Rabiner. A tutorial on hidden Markov models and selected applications in speech recognition. *Proceedings of the IEEE*, 77(2):257–286, 1989.
- [44] J. Chiang, Z. J. Wang, and M. J. McKeown. A hidden Markov, multivariate autoregressive (HMM-mAR) network framework for analysis of surface EMG (sEMG) data. *IEEE Transactions on Signal Processing*, 56(8): 4069–4081, 2008.
- [45] C. Li and S. V. Andersen. Efficient blind system identification of non-Gaussian autoregressive models with HMM modeling of the excitation. *IEEE Transactions on Signal Processing*, 55(6):2432–2445, 2007.
- [46] A. Zhan, M. A. Little, D. A. Harris, S. O. Abiola, E. R. Dorsey, S. Saria, and A. Terzis. High frequency remote monitoring of Parkinson’s disease via smartphone: Platform overview and medication response detection. *arXiv preprint arXiv:1601.00960*, abs/1601.00960, 2016.
- [47] J. Reilly, S. Dashti, M. Ervasti, J. D. Bray, S. D. Glaser, and A. M. Bayen. Mobile phones as seismologic sensors: Automating data extraction for the iShake system. *IEEE Transactions on Automation Science and Engineering*, 10(2):242–251, 2013.
- [48] J. J. Kavanagh, H. B. Menz, J. J. Kavanagh, and H. B. Menz. Accelerometry: A technique for quantifying movement patterns during walking. *Gait & Posture*, 28(1):1–15, 2008.
- [49] R. J. Hodrick and E. C. Prescott. Postwar U.S. business cycles: An empirical investigation. *Journal of Money, Credit and Banking*, 29(1):1–16, 1997.
- [50] S. Mallat. *A Wavelet Tour of Signal Processing: The Sparse Way*. Academic press, Burlington, Massachusetts, 2008.
- [51] M. A. Little and N. S. Jones. Generalized methods and solvers for noise removal from piecewise constant signals. I. Background theory. *Proceedings of the Royal Society of London A: Mathematical, Physical and Engineering Sciences*, 467(2135):3088–3114, 2011.
- [52] G. R. Arce. *Nonlinear Signal Processing: A Statistical Approach*. John Wiley & Sons, Inc., Hoboken, New Jersey, 2005.
- [53] B. U. Töreyn, E. B. Soyer, O. Urfalioğlu, and A. E. Cetin. Flame detection system based on wavelet analysis of PIR sensor signals with an HMM decision mechanism. In *2008 16th European Signal Processing Conference*, pages 1–5, 2008.
- [54] E. L. Andrade, S. Blunsden, and R. B. Fisher. Hidden Markov models for optical flow analysis in crowds. In *18th International Conference on Pattern Recognition (ICPR’06)*, volume 1, pages 460–463, 2006.
- [55] P.-C. Chung and C.-D. Liu. A daily behavior enabled hidden Markov model for human behavior understanding. *Pattern Recognition*, 41(5):1572–1580, 2008.
- [56] D. Gao, M. K. Reiter, and D. Song. Behavioral distance measurement using hidden Markov models. In *Recent*

- Advances in Intrusion Detection: 9th International Symposium*, pages 19–40, 2006.
- [57] Y. P. Raykov, E. Ozer, G. Dasika, A. Boukouvalas, and M. A. Little. Predicting room occupancy with a single passive infrared (PIR) sensor through behavior extraction. In *Proceedings of the 2016 ACM International Joint Conference on Pervasive and Ubiquitous Computing*, pages 1016–1027, 2016.
- [58] H. Juang and L. R. Rabiner. Hidden Markov models for speech recognition. *Technometrics*, 33(3):251–272, 1991.
- [59] M. Gales and S. Young. The application of hidden Markov models in speech recognition. *Foundations and Trends in Signal Processing*, 1(3):195–304, 2007.
- [60] S. M. Oh, J. M. Rehg, T. Balch, and F. Dellaert. Learning and inferring motion patterns using parametric segmental switching linear dynamic systems. *International Journal of Computer Vision*, 77(1):103–124, 2008.
- [61] V. P. Jilkov and X.-L. Rong. Online Bayesian estimation of transition probabilities for Markovian jump systems. *IEEE Transactions on Signal Processing*, 52(6):1620–1630, 2004.
- [62] S. Goldwater and T. Griffiths. A fully Bayesian approach to unsupervised part-of-speech tagging. In *Proceedings of the 45th Annual Meeting of the Association of Computational Linguistics*, pages 744–751, 2007.
- [63] M. Johnson, D. K. Duvenaud, A. Wiltschko, R. P. Adams, and S. R. Datta. Composing graphical models with neural networks for structured representations and fast inference. In *Advances in Neural Information Processing Systems 29*, pages 2946–2954. 2016.
- [64] E. Fox, E. B. Sudderth, M. I. Jordan, and A. S. Willsky. Nonparametric Bayesian learning of switching linear dynamical systems. In *Advances in Neural Information Processing Systems 21*, pages 457–464. 2009.
- [65] Y. W. Teh, M. I. Jordan, M. J. Beal, and D. M. Blei. Sharing clusters among related groups: Hierarchical Dirichlet processes. In *Advances in Neural Information Processing Systems 17*, pages 1385–1392. 2005.
- [66] M. J. Beal, Z. Ghahramani, and C. E. Rasmussen. The infinite hidden Markov model. In *Advances in Neural Information Processing Systems 14*, pages 577–584. 2002.
- [67] M. Aoki and A. Havenner. State space modeling of multiple time series. *Econometric Reviews*, 10(1):1–59, 1991.
- [68] D. J. Hand and K. Yu. Idiot’s Bayes – not so stupid after all? *International Statistical Review*, 69(3):385–398, 2001.
- [69] S. O. Abiola, K. M. Biglan, E. R. Dorsey, D. A. Harris, M. A. Little, S. Saria, and A. Zhan. Smartphone-PD: Preliminary results of an mHealth application to track and quantify characteristics of Parkinson disease in real-time. *Movement Disorders*, 30(10):6–7, 2015.
- [70] M. C. Hughes, W. T. Stephenson, and E. Sudderth. Scalable adaptation of state complexity for nonparametric hidden Markov models. In *Advances in Neural Information Processing Systems 28*, pages 1198–1206. 2015.
- [71] Y. P. Raykov, A. Boukouvalas, and M. A. Little. Simple approximate MAP inference for Dirichlet processes mixtures. *Electronic Journal of Statistics*, 10(2):3548–3578, 2016.
- [72] C. Leech, Y. P. Raykov, E. Ozer, and G. V. Merrett. Real-time room occupancy estimation with Bayesian machine learning using a single PIR sensor and microcontroller. In *2017 IEEE Sensors Applications Symposium (SAS)*, pages 1–6, 2017.
- [73] M. Pavel, T. Hayes, I. Tsay, D. Erdogmus, A. Paul, N. Larimer, H. Jimison, and J. Nutt. Continuous assessment of gait velocity in Parkinson’s disease from unobtrusive measurements. In *2007 3rd International IEEE/EMBS Conference on Neural Engineering*, pages 700–703, 2007.
- [74] L. R. Martin, S. L. Williams, K. B. Haskard, and M. R. DiMatteo. The challenge of patient adherence. *Therapeutics and Clinical Risk Management*, 1(3):189–199, 2005.